

---

# Tackling the Non-IID Issue in Heterogeneous Federated Learning by Gradient Harmonization

---

**Xinyu Zhang**  
Nanjing University  
xinyuzhang@smail.nju.edu.cn

**Weiyu Sun**  
Nanjing University  
weiyusun@smail.nju.edu.cn

**Ying Chen**  
Nanjing University  
yingchen@nju.edu.cn

## Abstract

Federated learning (FL) is a privacy-preserving paradigm for collaboratively training a global model from decentralized clients. However, the performance of FL is hindered by non-independent and identically distributed (non-IID) data and device heterogeneity. In this work, we revisit this key challenge through the lens of gradient conflicts on the server side. Specifically, we first investigate the gradient conflict phenomenon among multiple clients and reveal that stronger heterogeneity leads to more severe gradient conflicts. To tackle this issue, we propose FedGH, a simple yet effective method that mitigates local drifts through Gradient Harmonization. This technique projects one gradient vector onto the orthogonal plane of the other within conflicting client pairs. Extensive experiments demonstrate that FedGH consistently enhances multiple state-of-the-art FL baselines across diverse benchmarks and non-IID scenarios. Notably, FedGH yields more significant improvements in scenarios with stronger heterogeneity. As a plug-and-play module, FedGH can be seamlessly integrated into any FL framework without requiring hyperparameter tuning.

## 1 Introduction

Under the prevalence of large deep-learning models [Radford et al., 2018, Dosovitskiy et al., 2020], the demand for massive data overgrows. However, these datasets are usually dispersed across heterogeneous devices (e.g., mobile devices, personal computers, company servers, etc.), and conventional centralized training is constrained due to privacy concerns [Abadi et al., 2016, Kaissis et al., 2020, Geiping et al., 2020]. In this scenario, federated learning (FL) [McMahan et al., 2017], a privacy-preserving distributed training strategy, has emerged as a promising alternative. FL aims to collaboratively learn a global model based on multiple clients without data sharing. Specifically, each communication round in FL can be divided into three steps [McMahan et al., 2017]. First, clients download the global model to update the local one. Next, each client performs local training and uploads the local model. Finally, the server aggregates local models and updates the global model. Driven by the growing need for privacy protection and decentralized training, FL has been applied widely, including but not limited to face recognition [Niu and Deng, 2022], semantic segmentation [Miao et al., 2023], medical image analysis [Jiang et al., 2022], and wireless communication [Yan et al., 2022].

Despite its advanced characteristics, FL suffers from local drifts [Karimireddy et al., 2020] across multiple clients due to the non-independent and identically distributed (non-IID) issue, as illustrated

in Fig. 1. In homogenous scenario (Fig. 1b), each client has a similar local objective function due to the IID data and homogenous devices. As a result, the global update follows a similar optimization direction as observed in centralized training (Fig. 1a). Unfortunately, in practice, individual clients in FL often exhibit significant heterogeneity, as depicted in Fig. 1c. First, *Heterogenous data* induces diverse local optimization directions, straying from global minima [Karimireddy et al., 2020]. Moreover, *heterogeneous devices* (e.g., client 3 in Fig. 1c) with varying computational speeds and communication capacities exacerbate the situation [Li et al., 2020], leading to decreased convergence rate and compromised performance. Recently, corresponding solutions have been proposed to address the non-IID issue from different FL steps, including regularization [Li et al., 2020, Acar et al., 2021, Shi et al., 2022], contrastive learning [Li et al., 2021], variance reduction [Karimireddy et al., 2020] during local training, and normalized averaging [Wang et al., 2020b], momentum update [Hsu et al., 2019, Wang et al., 2019a, Reddi et al., 2020] during server aggregation. Additionally, personalized federated learning (pFL) methods [Huang et al., 2021, Ma et al., 2022] tackle the non-IID issue by training customized local model on each client. However, these methods are not aware of gradient conflicts across clients or investigate the relationship between the non-IID issue and the gradient conflict phenomenon in FL.

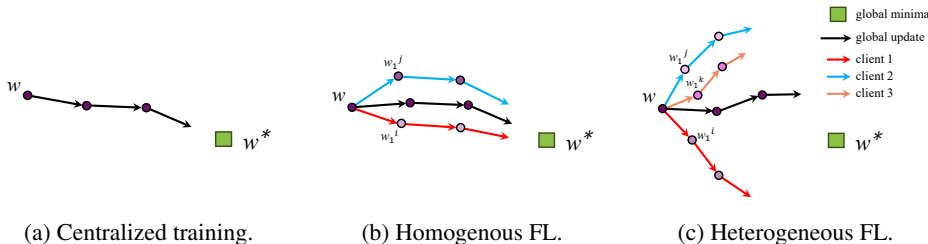


Figure 1: Illustration of optimization directions from centralized training, homogenous FL, and heterogeneous FL with gradient conflicts.

In this work, we propose FedGH, a simple yet effective method that addresses local drifts through Gradient Harmonization. Since the non-IID issue causes weight divergence [Zhao et al., 2018], we first study the gradient conflict phenomenon that emerges between local models on the server side. Intriguingly, we find that as the degree of local heterogeneity increases, the severity of gradient conflicts escalates. Motivated by this observation, we subsequently explore the mitigation of local drifts through gradient deconfliction. Specifically, if two gradients conflict, we execute a projection of one gradient onto the orthogonal plane of the other. This gradient harmonization strategy aims to enhance client consensus during server aggregation. Finally, we conduct extensive experiments on three widely used benchmarks, including CIFAR-10, CIFAR-100, and Tiny-ImageNet, with diverse degrees of non-IID challenge. Experimental results demonstrate that FedGH yields more performance boosting in more severe heterogeneous scenarios while maintaining a consistent improvement over multiple baselines [McMahan et al., 2017, Li et al., 2020, Wang et al., 2020b, Shi et al., 2022], including the latest state-of-the-art FedDecorr [Shi et al., 2022]. As a plug-and-play module, FedGH is easily integrated with any FL frameworks, requiring no hyperparameter tuning.

Our contributions in this work can be summarized as follows. First, we uncover that non-IID issue induces gradient conflicts between local models. Second, we propose a novel method called FedGH, which effectively mitigates local drifts via gradient harmonization during server aggregation. Third, we validate the efficacy of FedGH through comprehensive experiments, showcasing its consistent improvement over multiple baselines.

## 2 Related Works

### 2.1 Federated Learning

McMahan et al. [2017] propose a solid baseline in FL termed FedAvg, which directly averages local models to update the global model. However, Karimireddy et al. [2020] identify that FedAvg yields unstable and slow convergence in heterogeneous scenarios, and Li et al. [2020] further subdivide the

non-IID issue into systems heterogeneity and statistical heterogeneity. To tackle this key challenge, researchers have elaborated different strategies from different steps of FL.

During local training, many promising methods focus on regularizing the local objective. Specifically, [Li et al. \[2020\]](#) introduce a proximal term to minimize the gap between local and global models, while [Acar et al. \[2021\]](#) align these models via dynamic regularization. Additionally, [Li et al. \[2021\]](#) employ model-level contrastive learning to correct local updates, and [Shi et al. \[2022\]](#) tackle the non-IID issue from the dimensional collapse perspective. Moreover, the pursuit of flatter local minima is explored in [Qu et al. \[2022\]](#) and [Caldarola et al. \[2022\]](#) by applying a sharpness-aware optimizer.

On the server side, aggregation of local models and updating of the global model are two directions for addressing the non-IID problem. [Wang et al. \[2020b\]](#) propose a normalized averaging scheme instead of the naïve aggregation in FedAvg. In addition, [Wang et al. \[2020a\]](#) and [Ma et al. \[2022\]](#) aggregate local models in a layer-wise manner, while [Uddin et al. \[2022\]](#) introduce an outlier pruning strategy before aggregation. On the other hand, [Hsu et al. \[2019\]](#), [Wang et al. \[2019a\]](#), and [Reddi et al. \[2020\]](#) demonstrate that incorporating momentum-based updates into the global model is beneficial for mitigating local drift. However, our proposed FedGH is orthogonal to these methods and can be easily embedded in other FL frameworks.

## 2.2 Gradient Surgery

[Yu et al. \[2020\]](#) first identify that conflicting gradients lead to performance degradation in multi-task learning, introducing PCGrad to enhance optimization performance via gradient surgery. Subsequently, [Mansilla et al. \[2021\]](#) extend this insight to domain generation, presenting two gradient agreement strategies to alleviate gradient conflict. Moreover, DOHA introduce a sample-wise gradient deconfliction technique to boost generalization performance. In contrast, we uncover the gradient conflict phenomenon in FL caused by the non-IID issue. Our work centers on client-wise gradient harmonization during server aggregation rather than gradient surgery in every training iteration [[Yu et al., 2020](#), [Mansilla et al., 2021](#)]. Thus, FedGH is computationally efficient without introducing any extra communication costs.

## 3 Methodology

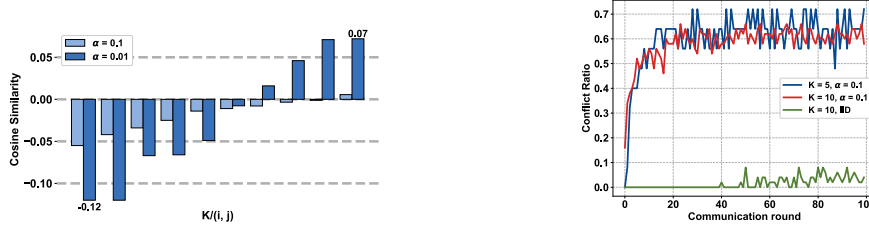
### 3.1 Problem Definition

FedGH aims to collaboratively learn a generalized model  $w$  from  $K$  clients over the dataset  $\mathcal{D} = \cup_{k \in [K]} \mathcal{D}_k$ . The global objective is  $\min_w L(w) = \sum_{k=1}^K \frac{n_k}{n} L_k(w)$ , where  $n = \sum_{k=1}^K n_k$  is the number of samples in  $\mathcal{D}$ . For client  $k$ ,  $L_k(w) = \mathbb{E}_{(x,y) \sim \mathcal{D}_k} \ell(w; (x, y))$ , where  $\mathcal{D}_k$  is the local dataset. Noteworthy, data is typically non-IID among  $K$  clients and cannot be shared due to privacy constraints.

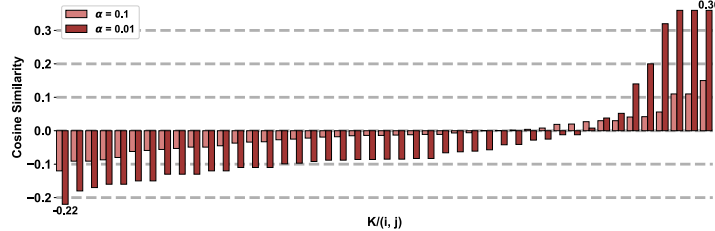
### 3.2 Gradient Conflict in Heterogeneous FL

We first probe the gradient conflict phenomenon under different degrees of non-IID. Toward this end, we first simulate the non-IID data among different clients using the Dirichlet distribution [[Hsu et al., 2019](#)]. Specifically, we sample  $P_c \sim \text{Dir}_K(\alpha)$  and allocate a  $p_c^k$  proportion of the samples of class  $c$  to client  $k$ . Here,  $\alpha$  denotes the concentration parameter, with smaller values indicating stronger heterogeneity. In non-IID scenarios, we set  $\alpha \in \{0.01, 0.1\}$ , and also set  $\alpha = \infty$  to simulate the IID scenario. Then, we implement FedAvg [[McMahan et al., 2017](#)] to train a convolutional neural network (CNN) utilized in [[Reddi et al., 2020](#)] on the CIFAR-10 dataset. Assuming that each client has uploaded the local model at the  $t$ -th communication round, we calculate the average gradient vector  $G_t = (g_t^1, g_t^2, \dots, g_t^K)$  during the local training period. The occurrence of gradient conflict is identified when the cosine similarity between  $g_t^i$  and  $g_t^j, \forall j \neq i$  becomes negative, i.e.,  $g_t^i \cdot g_t^j < 0$ .

First, we run 100 communication rounds involving 5 clients within two distinct non-IID scenarios. Subsequently, we visualize the sorted gradient similarity between each pair of clients in the final round, as illustrated in Fig. 2a. Our observation reveals the presence of gradient conflicts in heterogeneous settings, while a stronger heterogeneity results in a more severe conflict, as evidenced by the minimum similarity decreasing from -0.06 to -0.12. Next, we increase the number of clients to 10; the results are presented in Fig. 2c. We find that a larger number of clients further exacerbates the gradient



(a) Sorted similarity of gradient vectors between 5 clients. (b) Gradient conflict ratio during training.



(c) Sorted similarity of gradient vectors between 10 clients.

Figure 2: The non-IID issue causes gradient conflicts among (a) 5 and (c) 10 clients, with  $\alpha = 0.1$  and  $0.01$ , respectively. The  $x$ -axis is client index pairs, while the  $y$ -axis shows cosine similarity between gradient vectors. The change in gradient conflict ratio during training is depicted in (b).

conflict phenomenon, indicated by the reduction in minimum similarity from  $-0.12$  to  $-0.22$ . Finally, we compute the frequency of gradient conflicts occurring to unveil the variation of the gradient conflict over all communication rounds. We observe from Fig. 2b that as the training advances, gradient conflicts become more frequent. This phenomenon is consistent with the understanding that the non-IID issue causes local minima to deviate from global minima. Moreover, gradient conflict is widespread in FL, even within the IID setting, and becomes notably more severe in non-IID scenarios. These experiments demonstrate that stronger heterogeneity leads to more substantial local drifts, consequently inducing more violent gradient conflicts.

### 3.3 Tackling the Non-IID Issue by Gradient Harmonization

Motivated by intuitive insights on gradient conflicts in FL, we propose FedGH, a simple yet effective method, to tackle the non-IID issue by gradient harmonization. FedGH proceeds as follows: (1) First, FedGH recalculates average gradient vectors  $G_t = (g_t^1, g_t^2, \dots, g_t^K)$  based on uploaded local models  $W_t = (w_t^1, w_t^2, \dots, w_t^K)$ . For client  $k$ ,  $g_t^k = \frac{1}{\eta}(w_t^k - w_t)$ , where  $w_t$  is the global model and  $\eta$  is the learning rate. Note that gradients from distinct layers are flattened to a 1-d vector. (2) FedGH computes the cosine similarity between each gradient vector pair  $(g_t^i, g_t^j)$ ,  $\forall i \neq j$ . If the value is negative, indicating an obtuse angle between two gradient vectors, a gradient conflict between clients  $i$  and  $j$  is identified. (3) For each conflicting gradient pair  $(g_t^i, g_t^j)$ , FedGH executes harmonization by projecting  $g_t^i$  and  $g_t^j$  onto each other's orthogonal planes as follows:

$$\begin{aligned} g_t^i &\leftarrow g_t^i - \frac{g_t^i \cdot \tilde{g}_t^j}{\|\tilde{g}_t^j\|} \tilde{g}_t^j \\ g_t^j &\leftarrow g_t^j - \frac{g_t^j \cdot \tilde{g}_t^i}{\|\tilde{g}_t^i\|} \tilde{g}_t^i \end{aligned} \quad (1)$$

Where  $\tilde{G}_t = (\tilde{g}_t^1, \tilde{g}_t^2, \dots, \tilde{g}_t^K)$  is the deepcopy of  $G_t$ .

(4) Finally, local models  $W_t = (w_t^1, w_t^2, \dots, w_t^K)$  are updated using the adjusted gradients  $G_t = (g_t^1, g_t^2, \dots, g_t^K)$  derived from gradient harmonization. For client  $k$ ,  $w_t^k = w_t + \eta g_t^k$ . Subsequently, the server aggregates the updated local models to acquire the global model. The complete FedGH procedure is detailed in Algorithm 1.

The effectiveness of FedGH is illustrated in Fig. 3. In a scenario where the sum of two conflicting clients exhibits an optimization direction towards global minima, FedGH yields a faster convergence rate by discarding conflicting components of the gradient vector. Conversely, in cases where the optimization direction deviates from global minima, FedGH mitigates local drifts and rectifies the global update by enhancing local consensus across all clients. Moreover, compared with other notable methods [Li et al., 2020, Qu et al., 2022, Li et al., 2021], FedGH can be easily plugged into any FL framework without hyperparameter tuning or added communication costs. In our extensive experiments, we integrate FedGH with baselines that address the non-IID issue from local training [Li et al., 2020, Shi et al., 2022] and global aggregation [McMahan et al., 2017, Wang et al., 2020b]. Consistent performance boosting has been achieved on different benchmarks based on multiple baselines, proving the significance of minimizing gradient conflicts in FL.

---

**Algorithm 1:** Federated Averaging with **Gradient Harmonization (FedGH)**

---

**Input:** number of clients  $K$ , number of communication rounds  $T$ , learning rate  $\eta$ , local minibatch size  $B$ , number of local epochs  $E$

**Output:** global model  $w_T$

**Server executes:**

```

initialize  $w_0$ 
for each round  $t = 0, \dots, T - 1$  do
   $S_t \leftarrow$  (random set of  $K$  clients)
  for client  $k \in S_t$  in parallel do
     $w_{t+1}^k \leftarrow$  ClientUpdate( $k, w_t$ )
     $g_{t+1}^k \leftarrow \frac{1}{\eta}(w_{t+1}^k - w_t)$ 
   $\tilde{G}_{t+1} \leftarrow G_{t+1}$ 
  for  $k \in S_t$  do
    for  $j \in S_t \setminus k$  in random order do do
      if  $g_{t+1}^k \cdot \tilde{g}_{t+1}^j < 0$  then
         $g_{t+1}^k \leftarrow g_{t+1}^k - \frac{g_{t+1}^k \cdot \tilde{g}_{t+1}^j}{\|\tilde{g}_{t+1}^j\|^2} \tilde{g}_{t+1}^j$ 
       $w_{t+1}^k \leftarrow w_t + \eta g_{t+1}^k$ 
   $w_{t+1} \leftarrow \sum_{k \in S_t} \frac{n_k}{n} w_{t+1}^k$ 
return  $w_T$ 

```

**ClientUpdate**( $k, w_t$ ):

```

 $w_{t+1}^k \leftarrow w_t$ 
 $\mathcal{B} \leftarrow$  (split  $\mathcal{D}_k$  into batches of size  $B$ )
for local epoch  $i = 0, \dots, E - 1$  do
  for batch  $b \in \mathcal{B}$  do
     $w_{t+1}^k \leftarrow w_{t+1}^k - \eta \nabla \ell(w_{t+1}^k; b)$ 
return  $w_{t+1}^k$ 

```

---

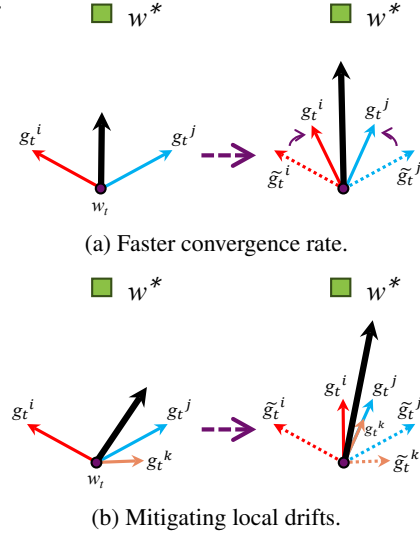


Figure 3: Illustration of FedGH’s effectiveness. If gradient conflict occurs between clients  $i$  and  $j$  in round  $t$ , FedGH projects  $g_t^i$  and  $g_t^j$  onto each other’s orthogonal planes. We highlight that FedGH yields a faster convergence rate in (a) while effectively mitigating local drifts from global minima in (b).

## 4 Experiments

### 4.1 Implementation Details

We reproduce four competitive FL baselines, including FedAvg [McMahan et al., 2017], FedProx [Li et al., 2020], FedNova [Wang et al., 2020b], and the state-of-the-art FedDecorr [Shi et al., 2022], based on the code implementation from Shi et al. [2022]. Noteworthy, FedProx and FedDecorr address the non-IID issue in the local training step, while FedNova and the proposed FedGH tackle it during the server aggregation step. To achieve optimal performance, we set  $\mu$  and  $\beta$  to 0.1 in FedProx and FedDecorr, respectively.

We conduct extensive experiments in three widely used benchmarks: CIFAR-10 (50,000 training samples, 10,000 test samples with 10 classes), CIFAR-100 (50,000 training samples, 10,000 test samples with 100 classes), and Tiny-ImageNet (100,000 training samples, 10,000 test samples with 200 classes). For CIFAR-10, we use a CNN model with two convolution layers [Reddi et al., 2020],

as mentioned in Sec. 3.2. For the more challenging CIFAR-100 and Tiny-ImageNet, we employ the MobileNetV2 [Sandler et al., 2018] as the backbone, following [Shi et al., 2022]. Our experiments are implemented on an NVIDIA GeForce RTX 3090 GPU using Pytorch 2.0.0. For all datasets, we partition the data into 20 clients with Autoaugment [Cubuk et al., 2018]. During local training, we use the SGD optimizer with a momentum of 0.9. The learning rate and the batch size are set to 0.01 and 64, respectively. We train each client for 5 local epochs and conduct 100 communication rounds for CIFAR-10 and CIFAR-100, and 50 communication rounds for Tiny-ImageNet, unless otherwise specified.

To validate the effectiveness of FedGH, we simulate multiple non-IID scenarios from cross-silo and cross-device perspectives [Reddi et al., 2020]. First, we generate *heterogeneous data* using the Dirichlet distribution detailed in Sec. 3.2. Specifically, for CIFAR-10, we disperse three datasets with  $\alpha \in \{0.1, 1.0\}$ . As for CIFAR-100 and Tiny-ImageNet, we set  $\alpha \in \{0.01, 0.1\}$ . Also, we follow [Zhuang et al., 2022, 2021] to split the dataset into  $K$  clients based on different classes, resulting in each client containing  $\frac{100}{K}$  and  $\frac{200}{K}$  classes for CIFAR-100 and Tiny-ImageNet, respectively. Moreover, we simulate *heterogeneous devices* by randomly selecting 20 out of 100 clients in each communication round, denoted as the client fraction  $C = 0.2$ .

## 4.2 Performance Boosting

Method	CIFAR-10 (%)			CIFAR-100 (%)		
	$\alpha = 0.1$ $C = 1.0$	$\alpha = 1.0$ $C = 0.2$	$\alpha = 1.0$ $C = 1.0$	$\alpha = 0.01$ $C = 1.0$	$\alpha = 0.1$ $C = 0.2$	$\alpha = 0.1$ $C = 1.0$
FedAvg	68.66	65.40	75.28	41.00	42.15	61.50
+ FedGH	<b>70.67</b>	<b>66.00</b>	<b>75.61</b>	<b>43.86</b>	<b>45.80</b>	<b>62.68</b>
FedProx	69.63	65.32	74.84	41.05	42.38	61.46
+ FedGH	<b>71.80</b>	<b>66.27</b>	<b>75.00</b>	<b>44.16</b>	<b>44.62</b>	<b>62.14</b>
FedNova	65.08	65.33	75.75	39.72	43.13	62.01
+ FedGH	<b>67.56</b>	<b>66.15</b>	<b>75.97</b>	<b>42.75</b>	<b>44.66</b>	<b>62.96</b>
FedDecorr	61.04	61.61	69.50	47.32	45.51	62.14
+ FedGH	<b>60.61</b>	<b>62.71</b>	<b>70.33</b>	<b>49.21</b>	<b>47.59</b>	<b>62.88</b>

Table 1: Top-1 test accuracy on the CIFAR-10 and CIFAR-100 datasets under multiple non-IID scenarios. All results are reported from the last communication round, and the highest accuracy in each scenario is highlighted in **Bold**.

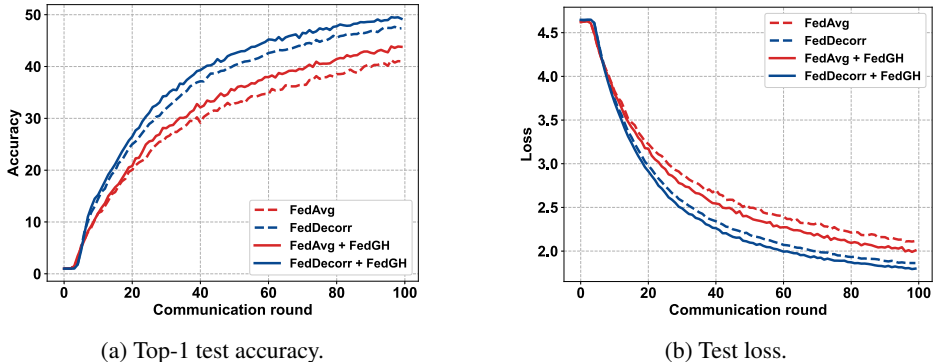


Figure 4: (a) Top-1 test accuracy and (b) test loss of the global model at each communication round in CIFAR-100, where  $\alpha = 0.01$ .

Tab. 1 demonstrates the top-1 test accuracy on CIFAR-10 and CIFAR-100 datasets under various non-IID scenarios. Noteworthy, we fix the random seed for fair comparison, and all results are



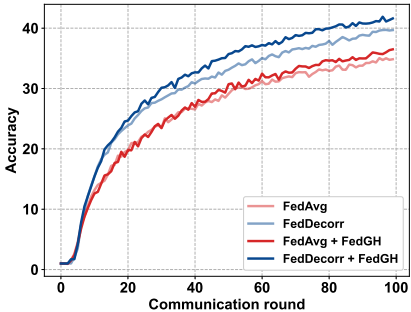
reported from the last communication round. We can observe that FedGH consistently improves all FL baselines across diverse heterogeneous settings. Specifically, (1) FedGH improves different backbones. We use a simple CNN model for CIFAR-10 and the more complex MobileNetV2 for CIFAR-100. The improvements observed on both datasets underscore the effectiveness of FedGH across different backbones. (2) FedGH improves multiple baselines. Each column in Tab. 1 shows the results of incorporating FedGH into different FL baselines. When integrated with different FL baselines, FedGH achieves substantial performance gains. For instance, on CIFAR-10, FedGH enhances FedNova and FedProx by 2.48% and 2.17%, respectively. In CIFAR-100, FedGH improves 3.11% and 3.03% with FedNova and FedProx. Notably, FedGH boosts the latest FedDecorr by up to 2.08%, demonstrating its significant performance and generalizability. (3) FedGH achieves greater performance enhancement in more severe non-IID scenarios. Each row in Tab. 1 corresponds to a distinct non-IID scenario. A similar trend can be observed in CIFAR-10 and CIFAR-100, where FedGH yields more substantial improvements in cases of stronger heterogeneity (i.e., smaller  $\alpha$  and  $C$ ). This trend results in a 0.16%  $\sim$  1.18% enhancement in less severe heterogeneity and a 1.89%  $\sim$  3.11% improvement in the strongest heterogeneous scenario. This effect can be attributed to the fact that stronger heterogeneity leads to more severe gradient conflicts among clients, as discussed in Section 3.2.

Tab. 2 presents the top-1 test accuracy achieved on the Tiny-ImageNet dataset. A consistent pattern emerges, demonstrating that FedGH consistently enhances performance across different baselines, with a more pronounced improvement in more severe non-IID scenarios. In particular, FedGH results in a 0.73% to 1.53% enhancement on FedDecorr across various degrees of heterogeneity and leads to a 2.07% improvement on FedNova when  $\alpha = 0.01$ . These experimental results demonstrate the efficacy of addressing the non-IID issue through gradient harmonization.

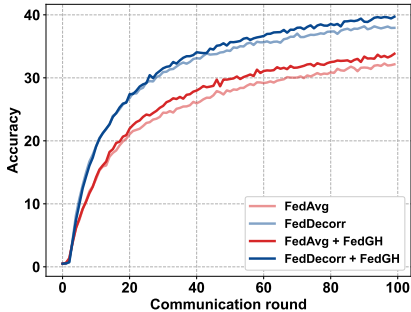
Furthermore, we visualize the test accuracy of the global model at each communication round in Fig. 4. It is evident that the incorporation of FedGH results in accelerated convergence and heightened performance. Moreover, FedGH achieves comparable performance with reduced communication rounds: 75% for FedAvg and 78% for FedDecorr, highlighting its capacity to enhance performance while significantly improving communication efficiency.

Method	Tiny-ImageNet (%)		
	$\alpha = 0.01$ $C = 1.0$	$\alpha = 0.1$ $C = 0.2$	$\alpha = 0.1$ $C = 1.0$
FedAvg	31.44	25.98	46.64
+ FedGH	32.94	26.28	47.45
FedProx	31.42	25.91	46.67
+ FedGH	32.83	26.58	47.23
FedNova	30.96	25.65	46.52
+ FedGH	33.03	26.74	47.13
FedDecorr	36.36	29.76	47.87
+ FedGH	<b>37.89</b>	<b>30.31</b>	<b>48.60</b>

Table 2: Top-1 test accuracy on the Tiny-ImageNet under multiple non-IID scenarios. All results are reported from the last communication round, and the highest accuracy in each scenario is highlighted in **Bold**.



(a) Top-1 accuracy in CIFAR-100, where each client contains 5 classes.



(b) Top-1 accuracy in Tiny-ImageNet, where each client contains 10 classes.

Figure 5: Top-1 test accuracy on the (a) CIFAR-100 and (b) Tiny-ImageNet datasets, where datasets are split into 20 clients based on different classes.

Finally, in addition to Dirichlet distribution-based heterogeneity, we partition the dataset into  $K$  clients based on different classes, following the setting described in Sec. 4.1. In this scenario, we train 20 clients with 100 communication rounds, where each client contains 5 and 10 classes in CIFAR-100 and Tiny-ImageNet, respectively. Fig. 5 illustrates that incorporating FedGH leads to a faster convergence rate and higher performance, especially when the baseline is the state-of-the-art FedDecorr. This enhancement amounts to a 1.93% improvement in CIFAR-100 and a 1.77% increase in Tiny-ImageNet over FedDecorr in the last communication round. Experimental results demonstrate that as a plug-and-play module, FedGH requires no hyperparameter tuning, making it straightforward to incorporate into diverse supervised or unsupervised FL frameworks [Zhuang et al., 2021, 2022, Han et al., 2022], as well as various deep-learning tasks.

### 4.3 Ablation study on the number of clients

As discussed in Sec. 3.2, having more clients increases the occurrences of gradient conflicts. Thus, we investigate the effectiveness of FedGH with different numbers of clients ( $K$ ) to determine whether it yields greater performance improvements with more clients. All experiments follow the same settings as presented in Sec. 4.1 and results are reported from the last communication round. We test FedGH in conjunction with FedAvg under the challenging non-IID scenario, where  $\alpha$  is set to 0.1 and 0.01 for CIFAR-10 and CIFAR-100, respectively. As shown in Tab. 3, it is evident that FedGH has only a slight impact on the baseline when  $K = 5$ . However, FedGH significantly enhances FedAvg as  $K$  increases, resulting in a 2.01% ~ 2.49% improvement in CIFAR-10 and 0.72% ~ 4.05% in CIFAR-100. Furthermore, we observe that FedGH achieves the most substantial performance improvement with the highest number of clients in CIFAR-100, demonstrating the scalability of FedGH. This observation also underscores that FedGH is particularly suitable for cross-device FL scenarios involving a large number of clients [Qu et al., 2022].

$K$	Method	CIFAR-10	CIFAR-100
5	FedAvg	64.93	62.93
	+ FedGH	64.75	63.14
10	FedAvg	69.74	56.12
	+ FedGH	72.23	56.84
20	FedAvg	68.66	41.00
	+ FedGH	70.67	43.86
30	FedAvg	67.21	32.16
	+ FedGH	67.04	36.21

Table 3: Top-1 test accuracy with different number of clients  $K$ .  $\alpha$  is set to 0.1 and 0.01 for CIFAR-10 and CIFAR-100, respectively.

### 4.4 Ablation study on the number of local epochs

We also conduct an ablation study on the number of local epochs ( $E$ ) under the same non-IID scenario, as shown in Tab. 4. In CIFAR-10, we consistently observe performance improvements by FedGH from 0.86% to 2.76%. Additionally, when  $E$  is set to 15, each client is susceptible to overfitting in relatively small-scale heterogeneous data. Interestingly, FedGH maintains high performance compared to  $E = 10$ , while FedAvg exhibits a notable degradation. This suggests that FedGH can mitigate local drifts and correct the optimization direction towards global minima. In CIFAR-100, FedGH achieves the most significant performance improvements of 3.93% and 2.86% at  $E = 1$  and  $E = 5$ , respectively. Furthermore, FedGH consistently enhances FedAvg as the number of local epochs increases. These observations demonstrate that FedGH can expedite the convergence rate of the global model, especially when local training resources are limited, making it suitable for scenarios where local computing power is constrained [Wang et al., 2019b].

$E$	Method	CIFAR-10	CIFAR-100
1	FedAvg	57.45	29.49
	+ FedGH	58.55	33.42
5	FedAvg	68.66	41.00
	+ FedGH	70.67	43.86
10	FedAvg	69.56	45.01
	+ FedGH	70.42	45.54
15	FedAvg	67.86	44.33
	+ FedGH	70.62	45.34

Table 4: Top-1 test accuracy with different number of local epochs  $E$ .  $\alpha$  is set to 0.1 and 0.01 for CIFAR-10 and CIFAR-100, respectively.



## 5 Conclusion

The non-IID issue has become a key challenge as federated learning research progresses. In this work, we first investigate the gradient conflict phenomenon among multiple clients in FL. Then, we propose a simple yet effective method called FedGH to tackle the non-IID issue through gradient harmonization. FedGH can seamlessly integrate into any FL frameworks without hyperparameters tuning. Extensive experiments demonstrate that FedGH consistently improves multiple state-of-the-art baselines across different degrees of heterogeneity, indicating its potential for real-world applications.

## References

- Martin Abadi, Andy Chu, Ian Goodfellow, H Brendan McMahan, Ilya Mironov, Kunal Talwar, and Li Zhang. Deep learning with differential privacy. In *Proceedings of the 2016 ACM SIGSAC conference on computer and communications security*, pages 308–318, 2016. [1](#)
- Durmus Alp Emre Acar, Yue Zhao, Ramon Matas Navarro, Matthew Mattina, Paul N Whatmough, and Venkatesh Saligrama. Federated learning based on dynamic regularization. *arXiv preprint arXiv:2111.04263*, 2021. [2](#), [3](#)
- Debora Caldarola, Barbara Caputo, and Marco Ciccone. Improving generalization in federated learning by seeking flat minima. In *European Conference on Computer Vision*, pages 654–672. Springer, 2022. [3](#)
- Ekin D Cubuk, Barret Zoph, Dandelion Mane, Vijay Vasudevan, and Quoc V Le. Autoaugment: Learning augmentation policies from data. *arXiv preprint arXiv:1805.09501*, 2018. [6](#)
- Alexey Dosovitskiy, Lucas Beyer, Alexander Kolesnikov, Dirk Weissenborn, Xiaohua Zhai, Thomas Unterthiner, Mostafa Dehghani, Matthias Minderer, Georg Heigold, Sylvain Gelly, et al. An image is worth 16x16 words: Transformers for image recognition at scale. *arXiv preprint arXiv:2010.11929*, 2020. [1](#)
- Jonas Geiping, Hartmut Bauermeister, Hannah Dröge, and Michael Moeller. Inverting gradients-how easy is it to break privacy in federated learning? *Advances in Neural Information Processing Systems*, 33:16937–16947, 2020. [1](#)
- Sungwon Han, Sungwon Park, Fangzhao Wu, Sundong Kim, Chuhan Wu, Xing Xie, and Meeyoung Cha. Fedx: Unsupervised federated learning with cross knowledge distillation. In *European Conference on Computer Vision*, pages 691–707. Springer, 2022. [8](#)
- Tzu-Ming Harry Hsu, Hang Qi, and Matthew Brown. Measuring the effects of non-identical data distribution for federated visual classification. *arXiv preprint arXiv:1909.06335*, 2019. [2](#), [3](#)
- Yutao Huang, Lingyang Chu, Zirui Zhou, Lanjun Wang, Jiangchuan Liu, Jian Pei, and Yong Zhang. Personalized cross-silo federated learning on non-iid data. In *Proceedings of the AAAI conference on artificial intelligence*, volume 35, pages 7865–7873, 2021. [2](#)
- Meirui Jiang, Zirui Wang, and Qi Dou. Harmoff: Harmonizing local and global drifts in federated learning on heterogeneous medical images. In *Proceedings of the AAAI Conference on Artificial Intelligence*, volume 36, pages 1087–1095, 2022. [1](#)
- Georgios A Kaissis, Marcus R Makowski, Daniel Rückert, and Rickmer F Braren. Secure, privacy-preserving and federated machine learning in medical imaging. *Nature Machine Intelligence*, 2(6): 305–311, 2020. [1](#)
- Sai Praneeth Karimireddy, Satyen Kale, Mehryar Mohri, Sashank Reddi, Sebastian Stich, and Ananda Theertha Suresh. Scaffold: Stochastic controlled averaging for federated learning. In *International conference on machine learning*, pages 5132–5143. PMLR, 2020. [1](#), [2](#)
- Qinbin Li, Bingsheng He, and Dawn Song. Model-contrastive federated learning. In *Proceedings of the IEEE/CVF conference on computer vision and pattern recognition*, pages 10713–10722, 2021. [2](#), [3](#), [5](#)
- Tian Li, Anit Kumar Sahu, Manzil Zaheer, Maziar Sanjabi, Ameet Talwalkar, and Virginia Smith. Federated optimization in heterogeneous networks. *Proceedings of Machine learning and systems*, 2:429–450, 2020. [2](#), [3](#), [5](#)
- Xiaosong Ma, Jie Zhang, Song Guo, and Wenchao Xu. Layer-wised model aggregation for personalized federated learning. In *Proceedings of the IEEE/CVF conference on computer vision and pattern recognition*, pages 10092–10101, 2022. [2](#), [3](#)
- Lucas Mansilla, Rodrigo Echeveste, Diego H Milone, and Enzo Ferrante. Domain generalization via gradient surgery. In *Proceedings of the IEEE/CVF international conference on computer vision*, pages 6630–6638, 2021. [3](#)

- Brendan McMahan, Eider Moore, Daniel Ramage, Seth Hampson, and Blaise Aguera y Arcas. Communication-efficient learning of deep networks from decentralized data. In *Artificial intelligence and statistics*, pages 1273–1282. PMLR, 2017. 1, 2, 3, 5
- Jiaxu Miao, Zongxin Yang, Leilei Fan, and Yi Yang. Fedseg: Class-heterogeneous federated learning for semantic segmentation. In *Proceedings of the IEEE/CVF Conference on Computer Vision and Pattern Recognition*, pages 8042–8052, 2023. 1
- Yifan Niu and Weihong Deng. Federated learning for face recognition with gradient correction. In *Proceedings of the AAAI Conference on Artificial Intelligence*, volume 36, pages 1999–2007, 2022. 1
- Zhe Qu, Xingyu Li, Rui Duan, Yao Liu, Bo Tang, and Zhuo Lu. Generalized federated learning via sharpness aware minimization. In *International Conference on Machine Learning*, pages 18250–18280. PMLR, 2022. 3, 5, 8
- Alec Radford, Karthik Narasimhan, Tim Salimans, Ilya Sutskever, et al. Improving language understanding by generative pre-training. 2018. 1
- Sashank Reddi, Zachary Charles, Manzil Zaheer, Zachary Garrett, Keith Rush, Jakub Konečný, Sanjiv Kumar, and H Brendan McMahan. Adaptive federated optimization. *arXiv preprint arXiv:2003.00295*, 2020. 2, 3, 5, 6
- Mark Sandler, Andrew Howard, Menglong Zhu, Andrey Zhmoginov, and Liang-Chieh Chen. Mobilenetv2: Inverted residuals and linear bottlenecks. In *Proceedings of the IEEE conference on computer vision and pattern recognition*, pages 4510–4520, 2018. 6
- Yujun Shi, Jian Liang, Wenqing Zhang, Vincent YF Tan, and Song Bai. Towards understanding and mitigating dimensional collapse in heterogeneous federated learning. *arXiv preprint arXiv:2210.00226*, 2022. 2, 3, 5, 6
- Md Palash Uddin, Yong Xiang, John Yearwood, and Longxiang Gao. Robust federated averaging via outlier pruning. *IEEE Signal Processing Letters*, 29:409–413, 2022. doi: 10.1109/LSP.2021.3134893. 3
- Hongyi Wang, Mikhail Yurochkin, Yuekai Sun, Dimitris Papailiopoulos, and Yasaman Khazaeni. Federated learning with matched averaging. *arXiv preprint arXiv:2002.06440*, 2020a. 3
- Jianyu Wang, Vinayak Tantia, Nicolas Ballas, and Michael Rabbat. Slowmo: Improving communication-efficient distributed sgd with slow momentum. *arXiv preprint arXiv:1910.00643*, 2019a. 2, 3
- Jianyu Wang, Qinghua Liu, Hao Liang, Gauri Joshi, and H Vincent Poor. Tackling the objective inconsistency problem in heterogeneous federated optimization. *Advances in neural information processing systems*, 33:7611–7623, 2020b. 2, 3, 5
- Shiqiang Wang, Tiffany Tuor, Theodoros Salonidis, Kin K Leung, Christian Makaya, Ting He, and Kevin Chan. Adaptive federated learning in resource constrained edge computing systems. *IEEE journal on selected areas in communications*, 37(6):1205–1221, 2019b. 8
- Na Yan, Kezhi Wang, Cunhua Pan, and Kok Keong Chai. Performance analysis for channel-weighted federated learning in oma wireless networks. *IEEE Signal Processing Letters*, 29:772–776, 2022. 1
- Tianhe Yu, Saurabh Kumar, Abhishek Gupta, Sergey Levine, Karol Hausman, and Chelsea Finn. Gradient surgery for multi-task learning. *Advances in Neural Information Processing Systems*, 33: 5824–5836, 2020. 3
- Yue Zhao, Meng Li, Liangzhen Lai, Naveen Suda, Damon Civin, and Vikas Chandra. Federated learning with non-iid data. *arXiv preprint arXiv:1806.00582*, 2018. 2
- Weiming Zhuang, Xin Gan, Yonggang Wen, Shuai Zhang, and Shuai Yi. Collaborative unsupervised visual representation learning from decentralized data. In *Proceedings of the IEEE/CVF international conference on computer vision*, pages 4912–4921, 2021. 6, 8
- Weiming Zhuang, Yonggang Wen, and Shuai Zhang. Divergence-aware federated self-supervised learning. *arXiv preprint arXiv:2204.04385*, 2022. 6, 8